Conclusions

The catalytic importance of the trans-electronic effect in coenzyme B_{12} dependent mechanisms is questionable in light of the magnitude of the calculated effect on the Co–C reduced overlap population observed in the present model. Additionally, the slight Co–C weakening brought about by Co–N_{trans} lengthening could be virtually offset by the electronic effects resulting from any slight corrinoid pucker (conceivably brought about through the binding of coenzyme to apoenzyme) analogous to that modeled herein. In view of the observed activity of cobinamide coenzyme (coenzyme B_{12} less the distal nucleotide loop),[29] the theoretical and experimental importance of the trans-electronic effect, as well as the trans-steric effect, in the holoenzyme appears to diminish. Likewise, since these results suggest that simple corrinoid distortion about the central metal ion does not serve to weaken the organocobalt linkage on purely stereoelectronic grounds, any possible catalytically important corrinoid distortion likely involves Co–C activation brought about through straightforward steric interactions rather than underlying electronic effects. Indeed, recent experiments[30] demonstrate that in model compounds possessing phosphine ligands trans to the Co–C bond, organometallic dissociation is by far more dependent on steric bulk of the trans ligand rather than its basicity; the steric effect, albeit a trans-steric effect, nearly masks the electronic effect. Additionally, Halpern and colleagues propose a cis steric interaction between the 5′-deoxyadenosyl group and the corrinoid macrocycle to be responsible for the relatively low dissociation energy of the coenzyme.[7]

The importance of steric effects in coenzyme B_{12} and model systems is obvious from the results of these calculations as well as the experimental data. The Co–C overlap population, and hence the Co–C bond strength, reflect a sensitive dependence to the C–Co–N_{eq} angle. Also important is the approach of a steric "push", which not only could serve as the initial means for the angular distortion of the Co–C bond but also could serve in and of itself as an electronic effector, decreasing the Co–C overlap population by means of associated electronic effects. Steric interaction as calculated here serves to bring about significant antibonding interaction between the cobalt-bound carbon and the offending atom(s); in turn, the Co–C bonding population decreases, and in the model system it is only this linkage which is weakened by such an effect.

It appears that the Co–C linkage is electronically susceptible to the onset of steric crowding directed at the cobalt-bound carbon. It is therefore likely that steric interactions, very possibly inducing the angular distortion of the Co–C bond, and the accompanying electronic phenomena herein described are primarily responsible for the initial homolytic activation in enzymatic mechanisms dependent on coenzyme B_{12}.

Acknowledgment. This work was supported in part by NIH Grant GM 06920. The helpful comments of Prof. Jack Halpern are gratefully acknowledged, and one of us (D.W.C.) thanks AT&T Bell Laboratories for a doctoral fellowship.

(29) Kato, T. et al. *J. Vitaminol. Kyoto* **1964**, *10*, 89, cited in Toraya, T.; Fukui, S. "Structure-Function Relationship of Vitamin B_{12} Coenzyme in the Diol-Dehydrase System", in "Biomimetic Chemistry", Dolphin, D. et. al., Eds., American Chemical Society: Washington, 1980; Adv. Chem. Ser. No. 191.
(30) Ng, F. T. T.; Rempel, G. L.; Halpern, J. *Inorg. Chim. Acta* **1983**, *77*, L165.

Ab Initio MO Study of the Coordination Modes and Bonding Nature of Rh^I–N_2 Complexes

Shigeyoshi Sakaki,*[1a] Keiji Morokuma,[1b] and Katsutoshi Ohkubo[1a]

Contribution from the Department of Synthetic Chemistry, Faculty of Engineering, Kumamoto University, Kurokami, Kumamoto 860, Japan, and Institute for Molecular Science, Myodaiji, Okazaki 444, Japan. *Received March 29, 1984*

Abstract: An ab initio MO study of $RhCl(PH_3)_2L$ (L = η^1-end-on N_2, η^2-side-on N_2, C_2H_4, CO, HCN, HNC, and NH_3) is presented. Two coordination modes of N_2, η^1-end-on and η^2-side-on, are compared. Though both coordination modes have the similar degree of back-donative (Rh → N_2) interaction, the η^1-end-on mode receives much larger electrostatic stabilization and slightly larger donative (N_2 → Rh) stabilization, and as a result, the η^1-end-on mode is more stable than the η^2-side-on mode. The bonding nature and electronic structure of the η^1-end-on N_2 complex are also examined: The π-back-donative interaction contributes to the N_2 coordination more strongly than the σ-donation, and the relative importance of the π-back-donation to the σ-donation is larger in the N_2 coordination than in the coordination of similar ligands, such as CO, HCN, and HNC. The coordinate bond of Rh(I) complexes is compared with that of Ni(0) complex, and $RhCl(PH_3)_2$ is suggested to possess versatile ability to form coordinate bond with various ligands.

Since the first synthesis of $[Ru(NH_3)_5(N_2)]X_2$ (X = Cl, Br, or I),[2] many transition-metal dinitrogen complexes have been synthesized and investigated actively.[3] Interests found in the chemistry of dinitrogen complexes are summarized as follows: (1) How does the inert N_2 molecule coordinate to transition metal? (2) Why is the η^1-end-on N_2 coordination usually found but the η^2-side-on coordination not common? (3) How can the N_2 ligand be reduced to N_2H_4 (or further to NH_3) under mild condition?

Recently, several MO studies of N_2 complexes have been carried out. Veillard[4] and Hori et al.[5] reported that the η^1-end-on N_2 complex was more stable than the η^2-side-on N_2 complex, and Lauher and Hoffmann[6] discussed the condition allowing the η^2-side-on N_2 coordination. For η^1-end-on N_2 complexes, Murrell et al.[7a] showed that the electron distribution was very sensitive

(1) (a) Kumamoto University. (b) Institute for Molecular Science. (nb) Institute for Molecular Science.
(2) Allen, A. D.; Senoff, C. V. *Chem. Commun.* **1965**, 621.
(3) For example: (a) Taqui Khan, M. M.; Martell, A. E. "Homogeneous Catalysis by Metal Complexes"; Academic Press: New York, 1974; Vol. I, p 181. (b) Allen, A. D.; Harris, R. O.; Loescher, B. R.; Stevens, J. R.; Whiteley, R. N. *Chem. Rev.* **1973**, *73*, 11. (c) Sellmann, D. *Angew. Chem., Int. Ed. Engl.* **1974**, *13*, 639. (d) Chatt, J.; Leigh, G. J. *Angew. Chem., Int. Ed. Engl.* **1978**, *17*, 400. (e) Chatt, J., da Camara Pina, G. L. M., Richards, R. L., Eds. "New Trends in the Chemistry of Nitrogen Fixation"; Academic Press: London, 1980.

(4) Veillard, H. *Nouv. J. Chim.* **1978**, *2*, 215.
(5) Hori, K.; Asai, Y.; Yamabe, T. *Inorg. Chem.* **1983**, *22*, 3218.
(6) Lauher, J. W.; Hoffmann, R. *J. Am. Chem. Soc.* **1976**, *98*, 1729.

0002-7863/85/1507-2686$01.50/0

to the kinds of metals and ligands, and Ondrechen et al.[7b] proposed that the η^1-end-on N_2 coordinate bond was contributed from the significant σ-covalency and the strong π-back-donation. Also, Hori et al. have discussed the N_2 reduction on transition-metal complexes.[8] However, some problems concerning the above-mentioned coordination bond and coordination modes of N_2 remain unclear. For examples, (i) the η^1-end-on N_2 coordinate bond has been discussed in terms of the σ-donation and π-back-donation, like the Dewar–Chatt–Duncanson model proposed for the olefin coordination. In this regard, several experimental results, such as the relative stability of η^1-end-on and η^2-side-on modes, and ESCA[9] and dipole moment measurements,[10] have been explained by considering the σ-donation and π-back-donation. But, the nature of N_2 coordinate bond has not been made clear sufficiently; it has been ambiguous how the η^1-end-on N_2 coordinate bond is characterized in comparison with the other similar ligands such as CO, HCN, and HNC and what difference can be found between the η^2-side-on N_2 and the η^2-ethylene coordinate bonds. (ii) The electron distribution in the N_2 ligand has not yet been unambiguously examined: It has been believed that higher negative charge is present at the terminal N atom,[11] whereas some ab initio MO calculations have given the higher negative charge at the coordinating N atom.[7] Finally, (iii) no conclusive discussion has been presented for the reason why not the η^2-side-on but the η^1-end-on N_2 complex is usually found, whereas several authors have discussed the relative stability of the η^1-end-on and η^2-side-on coordination of N_2 in terms of the σ-donation and π-back-donation.[4-6]

In this work, an ab initio MO study of $RhCl(PH_3)_2L$ (L = η^1-end-on N_2, η^2-side-on N_2, CO, HCN, HNC, NH_3, and C_2H_4) is presented. These complexes are chosen here for the following reasons: (a) The $RhCl(PH_3)_2$ fragment is very versatile for coordination of various ligands.[12] Therefore, the N_2 coordination bond can be compared with the similar ligands, such as CO, HCN, and HNC, and is expected to be characterized clearly. (b) Two modes of N_2 coordination, the η^1-end-on and η^2-side-on, have been discussed in $RhCl(PH_3)_2(N_2)$, previously.[12,13] (c) Although the N–N distance of N_2 complexes is usually longer than that of the free N_2 molecule, the rather short N–N distance has been reported in Rh^I–N_2 complexes.[13] It is worthwhile to study theoretically the N–N distance of Rh^I–N_2 complexes. (d) Because the well-known Wilkinson complex is composed of Rh(I), a characterization of the Rh(I) coordinate bond is important in the chemistry of transition-metal complexes and their catalysis. Through this MO study, the authors hope to present a convincing discussion on the N_2 coordination modes and to characterize the N_2 coordinate bond and the Rh(I) coordinate bond, by comparing with bonds of similar ligands and Ni(0) complexes, respectively.

Computational Procedure

Ab initio LCAO SCF MO calculations[14] were carried out for the closed-shell (singlet) state, as it is known that a square-planar Rh(I) complex has $(4d)^8$ configuration and takes a closed-shell singlet in the ground state. The basis sets used were the 4-31G set for ligand atoms,[15] and the [6s5p4d] contracted set for the Rh atom.[16] This [6s5p4d] set was contracted from the (14s10p8d) primitive Gaussian set, which was modified from (14s8p7d) by deleting the most diffuse s-type function and adding an s-type (exponent = 0.20), two p-type (0.30 and 0.15), and a d-type (0.10) function.[17] s-type functions, arising from the totally symmetric linear combination of d-type functions, were removed from the basis set. This contracted basis set is double-ζ quality for valence s and p orbitals and triple-ζ quality for valence d orbital.

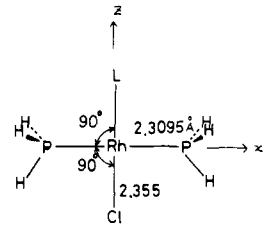

Figure 1. Coordinate system and assumed geometrical parameters of $RhCl(PH_3)_2L$ (L = η^1-end-on N_2, η^2-side-on N_2, CO, HCN, HNC, C_2H_4, or NH_3).

Scheme I

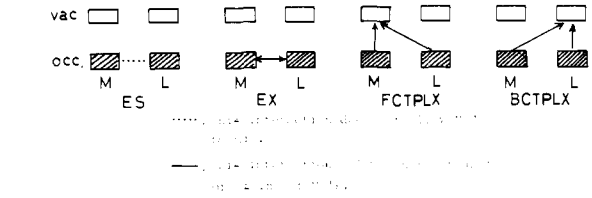

The energy decomposition analysis (EDA) was performed in order to investigate the coordinate bond nature in detail. The EDA scheme, reported elsewhere,[18] is briefly described here; the binding energy (BE) is defined as a stabilization of $RhCl(PH_3)_2L$ relative to $RhCl(PH_3)_2$ and L taking the respective equilibrium structures and is given as follows: BE = INT + DEF, where the interaction energy (INT) means the stabilization resulting from the interaction between $RhCl(PH_3)_2$ and L taking the deformed structures as in the complex, and the deformation energy (DEF) corresponds to the destabilization energy required to deform L from its equilibrium to the distorted structure. INT is further divided into various chemically meaningful interactions such as the electrostatic (ES), the exchange repulsion (EX), the forward charge transfer (FCTPLX), the back charge transfer (BCTPLX), and the higher order mixing term (R). These interactions included in the EDA are schematically shown in Scheme I: FCTPLX includes the charge transfer from L to $RhCl(PH_3)_2$, the polarization of $RhCl(PH_3)_2$, and their coupling terms. BCTPLX also includes the charge transfer from $RhCl(PH_3)_2$ to L, the polarization of L, and their coupling terms. Thus, FCTPLX and BCTPLX correspond to the donative and back-donative interactions, respectively.

Geometries and Their Optimization

$RhCl(PH_3)_2L$ has a square-planar structure, as shown in Figure 1. The Rh–Cl and Rh–P bond lengths were taken to be 2.3095 and 2.355 Å, respectively, by referring the structure of $RhCl(P\text{-}i\text{-}Pr_3)_2L$ (L = N_2 or C_2H_4).[12] Although the observed PRhCl angle differs slightly from 90°, this was assumed to be 90° for simplicity. The geometry of the PH_3 ligand was taken from the experimental structure of uncomplexed PH_3.[19a] These geometrical parameters

(7) (a) Murrell, J. N.; Al-Derzi, A.; Leigh, G. L.; Guest, M. F. *J. Chem. Soc., Dalton Trans.* **1980**, 1425. (b) Ondrechen, M. J.; Ratner, M. A.; Ellis, D. E. *J. Am. Chem. Soc.* **1981**, *103*, 1656.

(8) (a) Yamabe, T.; Hori, K.; Minato, T.; Fukui, K. *Inorg. Chem.* **1980**, *19*, 2154. (b) Yamabe, T.; Hori, K.; Fukui, K. *Inorg. Chem.* **1982**, *21*, 2046. (c) Yamabe, T.; Hori, K.; Fukui, K. *Inorg. Chem.* **1982**, *21*, 2816.

(9) (a) Finn, F.; Jolly, W. L. *Inorg. Chem.* **1972**, *11*, 1434. (b) Binder, H.; Sellmann, D. *Angew. Chem., Int. Ed. Engl.* **1973**, *12*, 1019. (c) Chatt, J.; Elson, C. M.; Hooper, N. E.; Leigh, G. J. *J. Chem. Soc., Dalton Trans.* **1975**, 2392.

(10) Darensbourg, D. J. *Inorg. Chem.* **1971**, *10*, 2399.

(11) Pombeiro, A. J. L., ref 3e, Chapter 6, p 153.

(12) Busetto, C.; D'Alfonso, A.; Maspero, F.; Perego, G.; Zazzeta, A. *J. Chem. Soc., Dalton Trans.* **1977**, 1828.

(13) (a) Hoffmann, P. R.; Yoshida, T.; Okano, T.; Otsuka, S.; Ibers, J. A. *Inorg. Chem.* **1976**, *15*, 2462. (b) Thorn, D. L.; Tulip, T. H.; Ibers, J. A. *J. Chem. Soc., Dalton Trans.* **1979**, 2022.

(14) IMSPACK Program for ab initio MO calculations was used, which consists of GAUSS70, HONDO, and many original routines (Morokuma, K.; Kato, S.; Kitaura, K.; Ohmine, I.; Sakai, S.; Obara, S. IMS Computer Program Library, The Institute for Molecular Science, 1980, Program 0372).

(15) Ditchfield, R.; Hehre, W. J.; Pople, J. A. *J. Chem. Phys.* **1971**, *54*, 724.

(16) Hyla-Kryspin, L.; Demuynck, J.; Strich, A.; Bénard, M. *J. Chem. Phys.* **1981**, *75*, 3954.

(17) The 14s primitives are contracted as groups of 6s, 2s, 2s, 1s, and 1s in a decreasing order of exponents with the contraction coefficients taken from ref 16. Similarly, the 10p and 8d primitives are grouped into 4p, 2p, 2p, 1p and 4d, 2d, 1d, 1d, respectively.

(18) (a) Morokuma, K. *Acc. Chem. Res.* **1977**, *10*, 294. (b) Kitaura, K.; Morokuma, K. *Int. J. Quantum Chem.* **1976**, *10*, 325. (c) Kitaura, K.; Sakaki, S.; Morokuma, K. *Inorg. Chem.* **1981**, *20*, 2292.

Table I. Optimized Geometrical and Experimental Parameters (Å)

complexes	opt	obsd	free ligand opt	free ligand obsd
$RhCl(PH_3)_2$-(η^1-N_2)	Rh–N = 2.06	1.970–1.885[13]		
	N–N = 1.08	1.074–0.958[13]	1.085[20]	1.094[19b]
$RhCl(PH_3)_2$-(η^2-N_2)	Rh–N = 2.70			
	N–N = 1.09			
$RhCl(PH_3)_2$-(C_2H_4)	Rh–C = 2.36	2.122[12]		
	C–C = 1.34	1.319[12]	1.316[15]	1.339[19b]
	θ^a = 7°			
$RhCl(PH_3)_2(CO)$	Rh–C = 1.94	1.85–1.77[21]		
	C–O = 1.13	1.123–1.14[21]	1.128[20]	1.1281[19b]
$RhCl(PH_3)_2$-(HNC)	Rh–C = 1.99			
	C–N = 1.16		1.162	1.165[b]
$RhCl(PH_3)_2$-(HCN)	Rh–N = 2.10			
	C–N = 1.14		1.140	1.156[19b]
$RhCl(PH_3)_2$-(NH_3)[c]	Rh–N = 2.22	2.23[19a]		

[a] The bending back angle of CH_2. [b] Cited in ref 20. [c] Optimization was carried out, for the experimental geometry of NH_3.

were fixed during optimization. The Rh–L distance and the geometry of L were optimized independently with each other. Two kinds of structures are possible in the η^2-side-on N_2 complex and C_2H_4 complex: in one, the η^2-N_2 and C_2H_4 are placed perpendicularly to the $RhCl(PH_3)_2$ molecular plane, and in another, they are placed in the $RhCl(PH_3)_2$ plane. In $RhCl(PH_3)_2(\eta^2$-$N_2)$ both structures were examined at N–N = 1.085 Å and Rh–N_2(the center of N_2) = 2.07 Å. The perpendicular structure is more stable than the in-plane structure by ca. 11 kcal/mol, perhaps due to the less steric repulsion and the stronger π-back-donation from Rh dπ to N_2; in fact, the N_2 electron population is larger in the perpendicular structure than in the in-plane structure by ca. 0.05e, and correspondingly the Rh dπ orbital population is less in the former than in the latter by ca. 0.05e. The C_2H_4 complex has been also reported experimentally to take a perpendicular structure.[12] Hereafter, only a perpendicular structure was examined in the η^2-N_2 and C_2H_4 complexes.

The optimized bond distances and bond angles are listed in Table I, compared with their experimental values and/or the geometrical parameters of free ligands. The Rh–L distances are overestimated by ca. 0.1 Å in the η^1-N_2 and CO complexes and by ca. 0.24 Å in the C_2H_4 complex, but excellent agreement was found between the calculated and experimental values of the Rh–NH_3 distance. The overestimation found in the Rh–N_2, Rh–CO, and Rh–C_2H_4 distances seems rather large at this level of calculation, and several reasons are considered: The first is the somewhat rough optimization technique; the Rh–L distance was varied by 0.1 Å keeping the $RhCl(PH_3)_2$ geometry fixed, and both Rh–L distance and geometry of L were optimized independently with each other. The potential curve with respect to the Rh–L distance is very shallow and the more detailed optimization would offer better results. The second is neglect of the electron correlation. The third is the missing of relativistic effect in MO calculation, which tends to yield rather long bond distances.[22] Although these factors are important, the large size of the examined complexes prevents us from carrying out further calculations. Nevertheless, the present results seem sufficient for qualitative discussion about coordination modes and bonding nature, because the relative stabilities of η^1-end-on and η^2-side-on modes were well reproduced by the present calculations. Further, the N–N and C–O distances calculated agree well with the experimental values. Both calculated and experimental N–N distances of the η^1-N_2 complex are slightly shorter than those corresponding to free N_2 molecule, and also the C–O distance is calculated to change little upon the coordination. This rather short N–N distance will be discussed later.

Results and Discussion

Coordination Modes: η^1-End-on vs. η^2-Side-on Modes: As shown in Table II, the η^1-end-on N_2 complex is more stable than the η^2-side-on complex by ca. 16 kcal/mol, and the η^2-side-on mode has very small binding energy. The difference in binding energy between two coordination modes is comparable with the activation enthalpy estimated for the intramolecular linkage isomerization of N_2 in $[Ru(NH_3)_5(N_2)]^{2+}$, where the isomerization is considered to proceed through the η^2-side-on structure.[23]

Now, let us examine why the η^1-end-on mode is more stable than the η^2-side-on mode. In the equilibrium structure, the η^2-side-on complex has small EX destabilization and small stabilization due to ES, FCTPLX, and BCTPLX, whereas the η^1-end-on mode suffers from large EX destabilization but receives large stabilization from ES, FCTPLX, and BCTPLX. This difference of energy characteristics between two modes comes from the fact that in the η^2-side-on mode the Rh–N_2 distance is much longer than in the η^1-end-on mode. To find the intrinsic difference between these two modes, we had better compare energy components at the same Rh–N_2 distance. However, it is difficult to define the same Rh–N_2 distance for the different coordination modes. Here, we consider the EX repulsion as a measure of "interfragment distance" between $RhCl(PH_3)_2$ and N_2 for the following reason:[24] the EX repulsion depends on contact of electron clouds between two fragments, $RhCl(PH_3)_2$ and N_2, and, therefore, the same EX value corresponds to the comparable interfragment distance. The EX value of the η^1-end-on N_2 complex (54.1 kcal/mol) is chosen as a standard for a comparison between the η^1-end-on and η^2-side-on modes, and the Rh–N_2 distance of the η^2-side-on mode is shortened to give this EX value. As shown in Table II, such a comparison offers a clear contrast between these two modes; although both coordination modes receive similar stabilization from BCTPLX, the η^1-end-on mode has much larger ES and slightly larger FCTPLX stabilizations than the η^2-side-on mode does. It is noted that BCTPLX, corresponding to the back-donative interaction, does not influence the relative stability of the two coordination modes, contrary to the suggestion of Hoffmann et al. that the d^n ($n > 4$) metal prefers the η^1-end-on N_2 coordination to the η^2-side-on mode, due to the larger π-back-donative interaction than that of the η^2-side-on mode.[6]

It is interesting to compare the η^2-side-on N_2 complex with the C_2H_4 complex, because C_2H_4, unlike N_2, can ligate to Rh(I) by way of η^2-side-on coordination to form a stable complex. Again, the comparison was carried out at the interfragment distance giving the same EX value (66.0 kcal/mol). As shown in Table II, the Rh-C_2H_4 complex is more stable than the η^2-side-on N_2 complex because of much larger ES and slightly larger FCTPLX interactions. These results suggest that the ES interaction seems to play a key role in determining the coordination modes of N_2. The ES potential map of N_2 is examined and shown in Figure 2A, where positive ES potential (given by dashed lines) means destabilization of a positive charge and negative ES potential (given by solid lines) means the stabilization. Apparently, the positive ES region expands perpendicularly to the N≡N bond, but the negative region expands toward the outside of N_2 bond along the N—N axis. This feature of ES potential, corresponding with the negative quadrupole moment of N_2,[25] comes from the sufficient electron accumulation on the lone pair region, enough to compensate ES repulsion due to charge of an N nucleus, but

(19) (a) Sutton, E. "Tables of Interatomic Distances and Configuration of Molecules and Ions"; Chemical Society: London, 1958. (b) Herzberg, G. "Molecular Spectra and Molecular Structure"; Van Nostrand Reinhold: New York, 1950; Vol. I, III.

(20) Binkley, J. S.; Pople, J. A.; Hehre, W. J. *J. Am. Chem. Soc.* **1980**, *102*, 939.

(21) (a) Dahl, L. F.; Martell, C.; Wampler, D. L. *J. Am. Chem. Soc.* **1961**, *83*, 1761. (b) Hoare, R. J.; Mills, O. S. *J. Chem. Soc., Dalton Trans.* **1972**, 2141.

(22) Ziegler, T.; Snijders, J. G.; Baerends, E. J. *J. Chem. Phys.* **1981**, *74*, 1271.

(23) Armor, J. A.; Taube, H. *J. Am. Chem. Soc.* **1980**, *92*, 2560.

(24) (a) Sakaki, S.; Kitaura, K.; Morokuma, K. *Inorg. Chem.* **1982**, *21*, 760. (b) Sakaki, S.; Kitaura, K.; Morokuma, K.; Ohkubo, K. *Inorg. Chem.* **1983**, *22*, 104.

(25) Buckingham, A. D. *Adv. Chem. Phys.* **1967**, *12*, 107.

(26) Similar discussion has been described by Kollman. Kollman, P. *J. Am. Chem. Soc.* **1977**, *99*, 4875.

Table II. BE, DEF, INT, and Energy Components between $RhCl(PH_3)_2$ and L (L = η^1-end-on N_2, η^2-side-on N_2, C_2H_4, CO, HCN, HNC, or NH_3) at Equilibrium Structure (kcal/mol)

		η^2-N_2							
L	C_2H_4	2.246[a]	2.70[b]	2.25[a]	η^1-N_2	CO	HNC	HCN	NH_3[c]
BE	−24.0	1.9	−5.7	0.0	−21.5	−35.8	−42.5	−26.5	−31.3
DEF	3.2	0.1	0.1	0.1	~0	~0	~0	~0	0[c]
INT	−27.2	1.8	−5.8	−0.1	−21.5	−35.8	−42.5	−26.5	−31.3
ES	−52.6	−26.7	−1.2	−21.4	−39.2	−90.7	−94.5	−47.9	−58.1
EX	66.0	66.0	7.1	54.1	54.1	121.5	111.5	52.7	50.1
FCTPLX	−16.2	−11.1	−4.1	−9.8	−13.0	−27.9	−26.2	−13.8	−15.4
BCTPLX	−17.6	−20.1	−4.6	−17.3	−17.7	−32.7	−25.5	−14.0	−5.7
R	−6.8	−6.3	−3.1	−5.7	−5.7	−6.1	−7.8	−10.0	−2.2

[a] The Rh–N_2 distance is shortened keeping the geometries of the other part fixed, to give the same EX value as that of the Rh–C_2H_4 or Rh–η^1-N_2 complex. [b] The equilibrium structure. [c] No optimization was carried out for the NH_3 part, because the 4-31G basis set gives poor results about the NH_3 geometry.

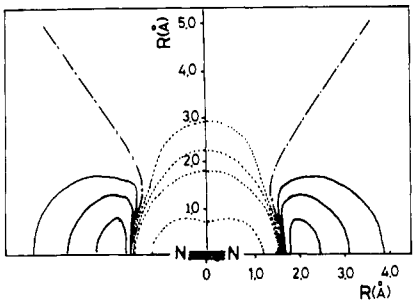

(A) ES potential map of N_2 [a)]

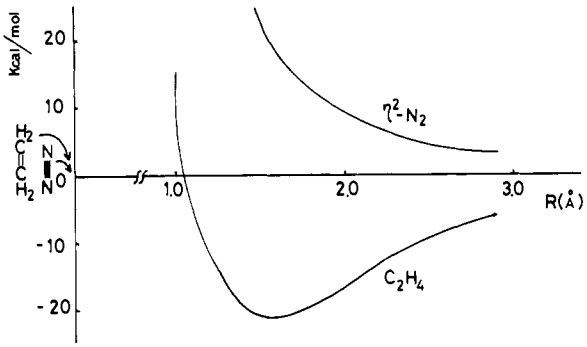

(B) ES potentials of η^2-N_2 and C_2H_4

Figure 2. ES potentials of N_2 and C_2H_4. (a) ±0.02, ±0.01, ±0.005, 0.0. (—) Negative value (stabilization of e^+); (- - -) positive value (destabilization of e^+); (-·-) 0.0.

insufficient electron accumulation on the π-orbtal region, not enough to compensate the ES repulsion due to charges of two N nuclei. This ES potential map indicates that the ES stabilization can be obtained when a positive metal ion such as Rh(I) approaches to N_2 along the N≡N bond axis, i.e., by way of η^1-end-on coordination, but that the ES destabilization would arise when a positive chemical species approaches to N_2 perpendicularly to the N≡N bond, i.e., by way of η^2-side-on coordination.[27] Then ES potentials of the η^2-side-on N_2 and C_2H_4 ligands are compared with each other, as shown in Figure 2B, where ES potentials are given as a function of distance from these ligands. Though the positive ES potential is observed for the η^2-N_2, the ES potential of C_2H_4 is negative in the region of coordinate bonding distance. This ES potential, corresponding with positive quadrupole moment of C_2H_4, is probably due to the negative charge of the C atom and the sufficient electron accumulation in the π-orbital region, enough to compensate charges of two C nuclei. Thus, the negative ES potential of C_2H_4 offers the large ES stabilization to the

(27) Actually, the negative ES interaction was obtained even in $RhCl(PH_3)_2(\eta^2$-$N_2)$. This is not strange, because the ES interactions also arise between the N_2 ES potential and $RhCl(PH_3)_2$ electron cloud and between the $RhCl(PH_3)_2$ ES potential and the N_2 electron cloud, which would lead to ES stabilization.

Table III. Changes in Mulliken Populations Caused by Various Interactions in $RhCl(PH_3)_2(\eta^1$-$N_2)$

	total	EX	FCTPLX	BCTPLX	*R*
Rh	−0.077	−0.005	0.004	−0.073	−0.003
4d	−0.118	−0.007	−0.045	−0.077	0.011
5sp	0.034	0.001	0.044	0.007	−0.018
N_2	0.078	0.0	−0.030	0.079	0.029
N_c[a]	0.051	−0.013	−0.035	0.057	0.042
N_t[b]	0.027	0.013	0.005	0.022	−0.013

[a] The coordinating N atom. [b] The terminal N atom.

Scheme II

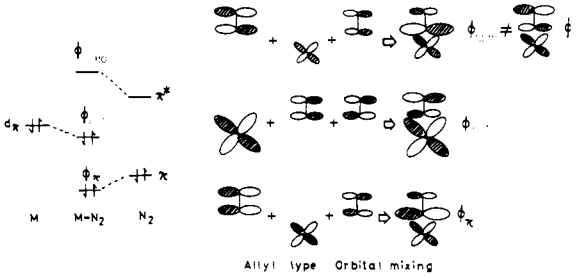

Rh^1–C_2H_4 complex, unlike the η^2-side-on N_2 complex. In other words, the ES potential favors the η^1-end-on N_2 and C_2H_4 complexes, but disfavors the η^2-side-on N_2 complex.

Now, the FCTPLX interaction should be discussed. This interaction depends on the energy and expanse of donor orbital. In the η^1-end-on N_2 coordination, the σ-lone pair orbital of N_2 plays a key role of a donor orbital, and in the η^2-side-on N_2 and C_2H_4 coordinations, the π-orbital is important as a donor orbital. Both the σ-lone pair and the π-orbitals of N_2 lie similarly in energy (σ-lone pair = −17.0 eV and π-orbital = −17.1 eV),[28] but due to hybridization, the σ-lone pair orbital extends toward Rh(I) more than the π-orbital does. Thus, FCTPLX stabilization is slightly larger in the η^1-end-on N_2 complex than in the η^2-side-on N_2 complex. The π-orbital of C_2H_4 (−10.1 eV) is higher in energy than that of N_2, leading to the larger FCTPLX stabilization of the C_2H_4 complex than that of the η^2-side-on N_2 complex.

In conclusion, the η^2-side-on N_2 complex is less stable than η^1-end-on N_2 and C_2H_4 complexes, mainly due to a smaller ES stabilization and secondarily due to a slightly smaller FCTPLX stabilization.

Bonding Nature and Electron Distribution of the η^1-End-on N_2 Complex. The bonding nature of the η^1-end-on N_2 complex will be investigated. As shown in Table II, the stabilization of BCTPLX is larger than that of FCTPLX, which is in accordance with the experimental results of ESCA[5] and dipole moment.[6] Electron distribution is given as Mulliken population (Table III) and difference density maps (Figure 3), where N_c represents the coordinating N atom and N_t is the terminal N atom. Although electron distribution based on the Mulliken population is slightly

(28) These orbital energies were calculated for the deformed structure of ligands as in the Rh(I) complexes.

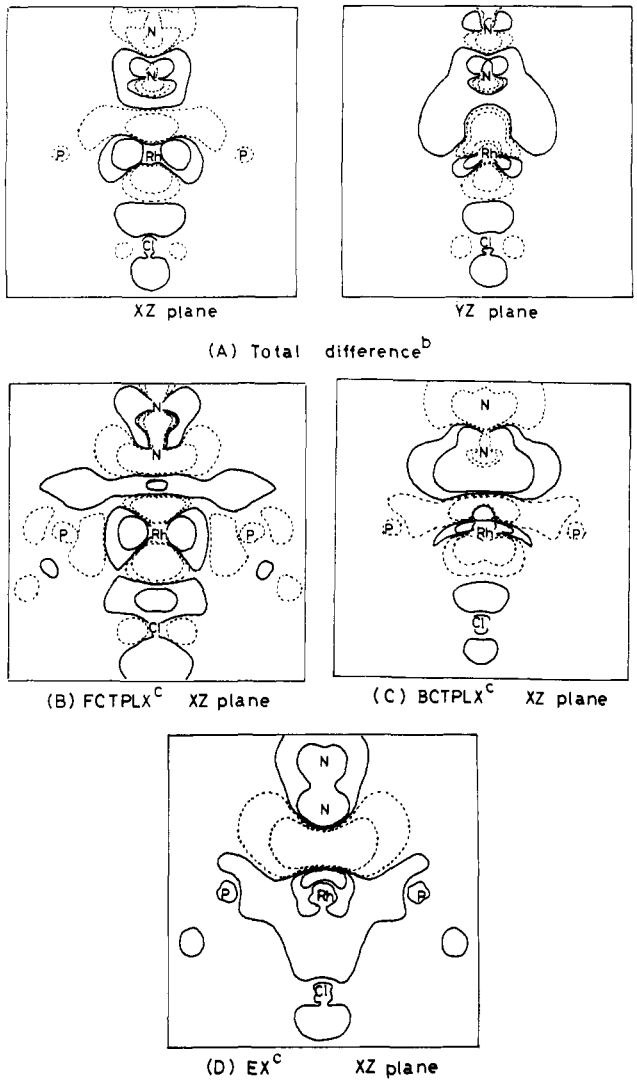

Figure 3. Difference density maps of $RhCl(PH_3)_2(\eta^1\text{-}N_2)$ (a) $[RhCl(PH_3)_2(\eta^1\text{-}N_2)]-[RhCl(PH_3)_2]-[N_2]$: (—) increased density, (---) decreased density. (b) Total difference density; ±0.005, ±0.0005. (c) FCTPLX, BCTPLX, and EX difference density; ±0.0001, ±0.001.

different from that based on the difference density map,[29] both Mulliken population and difference density map represent that N_c is more negatively charged than N_t. This result agrees with ab initio MO studies of $Ru(NH_3)_2(N_2)^{2+}$, $Mo(PH_3)_4(N_2)_2$, and $Fe(NH_3)_5(N_2)^{2+}$.[7] But in ESCA studies,[9] two peaks of N 1s ionization were observed and the higher N 1s binding energy was assigned to the N_c 1s ionization, suggesting that N_c was less negatively charged than N_t. Also in ab initio MO studies of $Mo(NH_3)_5(N_2)$ and $Cr(PH_3)_4(N_2)$[7a,8b] and EH-MO studies of several N_2 complexes,[6,30] N_t has been calculated to possess higher negative charge than N_c, which has been explained by allyl-type orbital mixing (Scheme II).[30] Here, the electron distribution of N_2 is examined in more detail through the component analysis of Mulliken population (Table III) and difference density maps (Figure 3B–D). The EX interaction pushes electron cloud to the terminal N_t atom, the FCTPLX interaction decreases electron population of the N_c atom, but the BCTPLX increases electron population of the N_c atom. Because the contribution of BCTPLX is the largest, the N_c atom is more negatively charged than the N_t atom.

(29) According to Mulliken populations, both N_c and N_t are negatively charged, but the difference density map suggests that N_t seems not to be negatively charged but to be slightly positively charged. This discrepancy is considered to come from the artificial picture of Mulliken population analysis when diffuse Gaussians are included in basis set.

(30) (a) Hoffmann, R.; Chen, M. M. L.; Thorn, D. L. *Inorg. Chem.* **1977**, *16*, 503. (b) DuBois, D. L.; Hoffmann, R. *Nouv. J. Chim.* **1977**, *1*, 479.

Table IV. Calculated N 1s Ionization Energy (eV)

	$RhCl(PH_3)_2(\eta^1\text{-}N_2)$			free N_2		
	Koopmans[a]	ΔSCF[a]	relaxatn energy	Koopmans	ΔSCF[a]	relaxatn energy
N_c	428.19	412.20	15.99	426.66	412.60	14.06
N_t	427.88	411.21	16.67			
ΔI_p[b]	0.31	0.99				

[a] See ref 32. [b] The difference between the N_c 1s and N_t 1s ionization energies.

In this connection, it is worth examining the allyl-type orbital mixing. As shown in Scheme II, the HOMO of $RhCl(PH_3)_2(N_2)$ mainly consists of Rh $d\pi$, with which the N_2 π^* orbital mixes in a bonding combination but the N_2 π-orbital interacts in an antibonding way.[31] Consequenty, the N_t p_π orbital contributes to the HOMO more than N_c p_π does. In fact, the HOMO given by the present MO calculation has the shape similar to HOMO shown in Scheme II. On the other hand, the Rh $d\pi$ and N_2 π^* orbitals mix into the more stable N_2 π-orbital in a bonding combination with each other, yielding the ϕ_π orbital (Scheme II), in which the contribution of N_c p_π orbital is larger than that of N_t p_π. These two MO's, HOMO and ϕ_π, result in different electron distribution of N_2; in the HOMO, N_t has more electron population, but in ϕ_π, N_c has more electron population. Thus, even if these occupied MO's are examined, it is difficult to reveal which of the two's, N_c or N_t, is more negatively charged. In such a case, examination of the virtual MO would give an answer. When the contribution of N_t p_π is larger than that of N_c p_π in the virtual space, electrons are accumulated on N_c more than on N_t and vice versa. The LUMO is the N_2 π^* orbital in main character. According to the orbital mixing rule,[31] Ru $d\pi$ and N_2 π orbitals mix into LUMO in an antibonding combination with each other, and, therefore, the LUMO should have a shape as shown in Scheme II. This shape requires that N_t is more negatively charged than N_c. However, the LUMO obtained by the present MO calculation is contributed from the N_t p_π orbital more than the N_c p_π orbital (Scheme II). The shape of calculated LUMO means that N_c is more negatively charged than N_t, as shown in Figure 3 and Table III, contrary to the allyl-type orbital mixing. Therefore, the orbital mixing seems unimportant, and other factors are expected to play a key role in determining the N_2 electron distribution of $RhCl(PH_3)_2(N_2)$. As a candidate of such factors, the positive charge of Rh(I) would be considered. This positive charge would polarize the N_2 electron cloud toward Rh(I), and N_c would be more negatively charged than N_t. In fact, BCTPLX, which increases the electron population of N_c, includes the polarization of the N_2 ligand as shown in Scheme I.

The above discussion also suggests that the electron distribution of N_2 is very sensitive to kinds of metals and ligands, as has been described,[11] because two factors, the orbital mixing and the positive charge of the central metal, cause different effects on the N_2 electron distribution: N_c is more negatively charged than N_t if the latter factor is more important, as in the case of complexes with highly charged central metal such as $Mo(PH_3)_4(N_2)_2$ (Mo = +0.65*e* Mulliken charge), $Fe(NH_3)_5(N_2)^{2+}$ (Fe = +1.50*e*), $Ru(NH_3)_5(N_2)^{2+}$ (Ru = +0.96*e*),[7] and $RhCl(PH_3)_2(N_2)$ (Rh = +0.49*e*), but N_t has larger electron population if the former is more important, as in the case of complexes with less charged central metal such as $Mo(NH_3)_5(N_2)$ (Mo = +0.40*e*).[7]

The next problem is ESCA assignment of N 1s ionization. Although no ESCA study has been reported for $RhCl(PH_3)_2(N_2)$, the higher N 1s binding has been usually assigned to the N_c 1s ionization in ESCA studies of N_2 complexes,[9] suggesting that N_c is less negatively charged than N_t, in conflict with the present calculated electron distribution. According to Koopmans theorem, however, the present MO calculation showed that the N_c 1s ionization was higher in energy than the N_t 1s ionization (Table IV).[28] Further, the N 1s ionization energy was calculated through

(31) Inagaki, S.; Fukui, K. *Chem. Lett.* **1974**, 509. Inagaki, S.; Fujimoto, H.; Fukui, K. *J. Am. Chem. Soc.* **1976**, *98*, 4054.

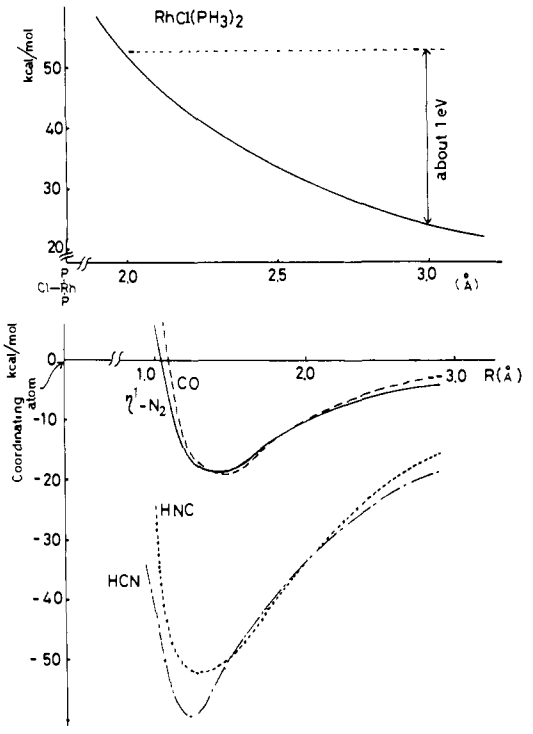

Figure 4. ES potentials of η^1-N_2, CO, HNC, HCN, and $RhCl(PH_3)_2$. Coordinating atom is placed at $R = 0.0$.

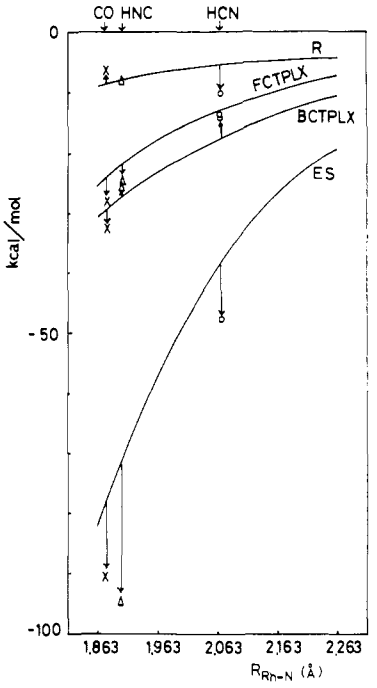

Figure 5. Energy components between $RhCl(PH_3)_2$ and η^1-N_2 vs. Rh–N distance. Energy components of the HCN, HNC, and CO complexes are plotted at the interfragment distance giving the same EX value.

ΔSCF technique by using the RHF–MO method;[32] apparently, the N 1s ionization potential of $RhCl(PH_3)_2(N_2)$ is lower in energy than that of the free N_2 molecule, and the N_c 1s ionization is higher in energy than the N_t 1s ionization (Table IV). A reason why a simple relation cannot be found between the N 1s ionization energy and the N electron population should be examined. Generally speaking, the core binding energy is equated to a term involving the net charge of the atom possessing the ionized core orbital plus the electrostatic potential due to the charges of all the other atoms minus the relaxation energy associated with the core ionization.[33a] If only the N atomic charge is considered, the N_c 1s ionization should be lower in energy than the N_t 1s ionization. However, the highly positive charge of Rh(I) leads to positive ES potential (destabilization of positive charge e^+), as shown in Figure 4. The ES potential at the position of ca. 2.0 Å (the position of N_c) is more positive than that at ca. 3.0 Å (the position of N_t), yielding a larger stabilization of N_c 1s electron than that of N_t 1s electron and, conversely, yielding a larger destabilization of the hole state on N_c 1s than that of N_t 1s. Relaxation energies, calculated here, are shown in Table IV; the N_t 1s ionization causes larger relaxation energy than the N_c 1s ionization does.[33b] The above discussion suggests that the Rh(I) positive charge and the relaxation energy increase the N_c 1s ionization energy more than the N_c negative charge lowers it, and, consequently, the N_c 1s ionization is higher in energy than the N_t 1s ionization. Therefore, present electron distribution does not contradict with the ESCA assignment,[34] and caution is necessary when the net charge is deduced from a ESCA chemical shift in a system containing charged atoms.

N≡N Bond Length and π-Back-Donation. The N≡N distance is calculated to change little by the coordination,[35] as shown in Table I, whereas the π-back-donation, leading to the N≡N bond lengthening, considerably contributes to the N_2 coordinate bond. Of course, the BCTPLX interaction, corresponding to the back-donation, weakens the N≡N bond, as shown by the difference density map of BCTPLX (Figure 3C), in which the electron density is reduced in the N≡N bonding region. The FCTPLX interaction, corresponding to donative interaction, also reduces the electron density in the N≡N bonding region. As a result, the total density is reduced in this region by coordination. Thus, both FCTPLX and BCTPLX are expected to lengthen the N≡N bond distance, and the rather short N≡N distance of the Rh^I–N_2 complex cannot be attributed to FCTPLX and BCTPLX interactions.

On the other hand, it is shown by the total difference density map that the N_c atom is negatively charged but the N_t atom seems to have slightly positive charge. This electron distribution would offer the electrostatic attraction between two N atoms, and the N≡N distance would be hardly lengthened in $RhCl(PH_3)_2(N_2)$.

Comparison of the Coordinate Bond between the η^1-End-on N_2 and the Other Ligands. Because HCN, HNC (models of CH_3CN and CH_3NC, respectively), and CO have a lone pair orbital and two sets of π and π* orbitals, these ligands can coordinate to metal through σ-donation of the lone pair electrons and π-back-donation into the π* orbitals, as N_2 does. It is worthwhile to characterize the coordinate bond of the η^1-end-on N_2 ligand by comparison with those of the similar ligands such as HCN, HNC, and CO. The binding energies (BE) between $RhCl(PH_3)_2$ and these ligands are given in Table II, from which the coordination is expected to become weak in the order HNC > CO > HCN > η^1-end-on N_2. First, the relative importance of σ-donation and π-back-donation is compared at the equilibrium structure: As shown in Table II, BCTPLX ~ 1.4FCTPLX in the η^1-end-on N_2 complex, BCTPLX ~ 1.2FCTPLX in the CO complex, and BCTPLX ~

(32) Kosugi, N.; Kuroda, H. *Chem. Phys. Lett.* **1980**, *74*, 490. In the SCF calculations, the GSCF2 program written by Kosugi, N. (Tokyo University), was used, in which the spherical d-oribtals arising from the totally symmetric linear combination of d-type orbitals were not excluded.

(33) (a) For example: Gelius, U. *Phys. Scr.* **1974**, *9*, 133. (b) The relaxation energy for the N_c 1s ionization would be expected to be larger than that for the N_t 1s ionization, because N_c directly interacts with the $RhCl(PH_3)_2$ part. The present calculation, however, shows the opposite trend. Through relaxation, many electrons flow into the p_π orbitals of the ionized N atom. The large relaxation for the N_t 1s ionization would be probably due to allyl-type orbital mixing, which accelerates such electron flow into the N_t p_π orbitals.

(34) Of course, in many studies, two peaks of N 1s ionization are considered to be due to the satelite of N 1s ionization. (For example: Freund, H. J.; Pulm, H.; Dick, B.; Lange, R. *Chem. Phys.* **1983**, *81*, 99.) Even so, it is not meaningless to reveal that the N 1s ionization potential cannot always be related to the electron population of N atom in the η^1-end-on N_2 complexes.

(35) The possibility that the thermal vibration incorrectly gives a rather short N–N distance cannot be neglected, as described in some experimental works.[13] However, from the present MO study, it seems intrinsic that the N–N distance is not lengthened so much in Rh^I–N_2 complex.

Table V. Ligand Properties: Mulliken Charge of the Coordinating Atom (MC) π, π^*, and Lone Pair Orbital Energies[a]

	HNC	CO	HCN	η^1-N_2	η^2-N_2	C_2H_4	NH_3
MC[b]	+0.30	+0.40	−0.34	0.0	0.0	−0.33	−0.92
			Orbital Energy (eV)				
π	−14.1	−17.4	−13.6	−17.1	−17.0	−10.1	
π^*	5.6	4.0	5.4	4.4	4.3	4.9	
lone pair	−13.0	−14.9	−15.6	−17.1	−17.1		−11.0

[a] For the distorted structure as in the total complex. [b] Mulliken charge of the coordinating atom.

FCTPLX in the other complexes. Thus, the back-donation is more important in the η^1-end-on N_2 complex than in the other ligands.

Now, each energy component will be examined in more detail. The energy components of the η^1-end-on N_2 complex were first obtained at several Rh–N_2 distances, and they are connected as the "reference curves", as shown in Figure 5. Then energy components of the other Rh–L complexes taking their optimized structures are plotted at the Rh–N_2 distance giving the same EX value as the Rh–L complex. Through such plots, the Rh–L coordinate bond is compared with that of the Rh–η^1-N_2 complex at the similar "interfragment distance"; in this comparison, if the energy component of the Rh–L complex is placed below the reference curve, it means that the Rh–L complex receives the larger stabilization from the interaction than the Rh–N_2 complex does and vice versa.[36] FCTPLX and BCTPLX of the CO complex are placed below the reference curves, as shown in Figure 5, indicating that the CO complex has stronger donating and back-donating interactions than the η^1-end-on N_2 complex. These strong FCTPLX and BCTPLX interactions apparently result from the higher orbital energy of the CO lone pair orbital and the lower orbital energy of the CO π^* orbital than the corresponding ones of N_2 (see Table V). The large ES stabilization of CO is also noted in Figure 5. At first glance, this large stabilization seems strange, because the coordinating C atom has positive Mulliken charge. However, CO has a lone pair electron that gives C^-O^+ polarity of σ-electrons, and this polarity is expected to lead to a significant ES stabilization with a positive Rh(I) ion. In fact, the CO ligand offers ES potential similar to that of N_2, in spite of the positively charged C atom, as shown in Figure 4. Also we should consider the situation that the CO and N_2 ligands are placed in the ES potential field of $RhCl(PH_3)_2$. The ES potential of $RhCl(PH_3)_2$, shown in Figure 4, is positive at the coordinating distance. Because the N nucleus charge is larger than the C nucleus charge, the ES potential of $RhCl(PH_3)_2$ more destabilizes the η^1-end-on N_2 coordination than the CO coordination. Consequently, the CO coordination bond is strong due to the large stabilizations of ES, FCTPLX, and BCTPLX.

Coordinate bonds of HCN and HNC receive a considerably larger ES and a slightly larger FCTPLX stabilization but a slightly smaller BCTPLX stabilization than that of η^1-end-on N_2 does. ES potentials of HNC and HCN are more negative than those of the η^1-end-on N_2 and CO ligands, as shown in Figure 4, perhaps due to the less positive (in HNC) or more negative (in HCN) Mulliken charge of the coordinating atom (see Table V). Thus, the ES stabilization is large in HCN and HNC coordinations. Also these ligands have the lone pair and π^* orbitals higher in energy than the η^1-end-on N_2 ligand does (Table V), leading to larger FCTPLX but smaller BCTPLX stabilizations of these complexes than those corresponding to the η^1-end-on N_2 complex. The strong ES and FCTPLX interactions result in the strong coordinate bonds of HCN and HNC. Of these two ligands, the lone pair orbital of HNC lies considerably higher in energy than that of HCN, and the coordinating C atom of HNC has less nucleus charge than the coordinating N atom of HCN, leading to a larger ES (consider the positive ES potential field of $RhCl(PH_3)_2$) and larger FCTPLX stabilizations of the HNC coordination. As a result, HNC is the strongest ligand for Rh(I).

In conclusion, the η^1-end-on N_2 coordination receives a weaker ES and FCTPLX stabilization than the other ligands, which seems a main factor for the weak coordination bond of N_2. The BCTPLX interaction of the η^1-end-on N_2 complex is not always stronger than the other ligands; for example, the CO complex possess the stronger BCTPLX than the η^1-end-on N_2 complex. However, the relative importance of BCTPLX to FCTPLX is larger in the N_2 coordination than in the coordination of the other ligands, and the strong Lewis basicity is required for the N_2 coordination.

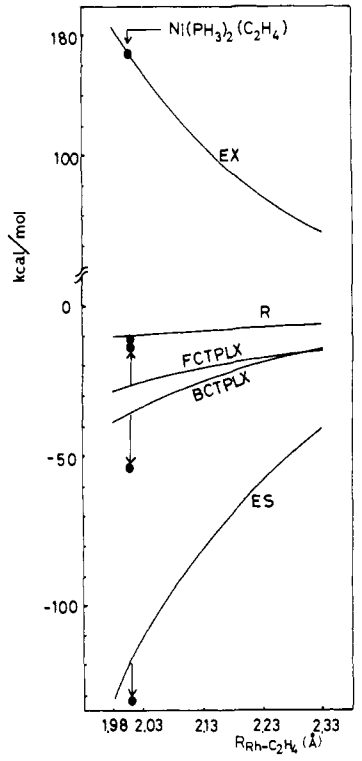

Figure 6. Energy components for $RhCl(PH_3)_2(C_2H_4)$ vs. Rh–C_2H_4 distance, where energy components for $Ni(PH_3)_2(C_2H_4)$ are plotted at the Rh–C_2H_4 distance giving the same EX value.

Comparisons between NH_3 and the Other Ligands and between the Rh(I) and Ni(0) Coordinate Bonds. It is interesting to investigate how differently the coordinate bond of non-Werner-type complexes is described from that of Werner-type complexes. Here, the NH_3 coordinate bond, usually found in Werner-type complexes, is compared with the coordinate bonds of N_2, CO, HCN, and HNC. A clear contrast is found in Table II; the NH_3 coordinate bond has larger ES stabilization than EX destabilization, whereas all of the other ligands suffer EX destabilization larger than ES stabilization. Another contrast is also found in BCTPLX; the NH_3 coordination receives much smaller BCTPLX stabilization, due to the absence of low-lying acceptor orbital, whereas the large BCTPLX is present in the coordination of the other ligands. The FCTPLX stabilization of NH_3 is less than those of CO and HNC but is almost the same degree as those of HCN and η^1-end-on N_2. These results suggest that the coordinate bond of Werner-type complexes would be characterized by large ES stabilization and small BCTPLX stabilization.

Then the Rh–C_2H_4 complex is compared with the Ni(0) complex, though the used basis set for Ni is slightly different from that of Rh.[18c,37] Energy components of the Rh–C_2H_4 complex

(36) A similar comparison has been carried out for various Ni(0) complexes, and successful discussion has been presented.[24]

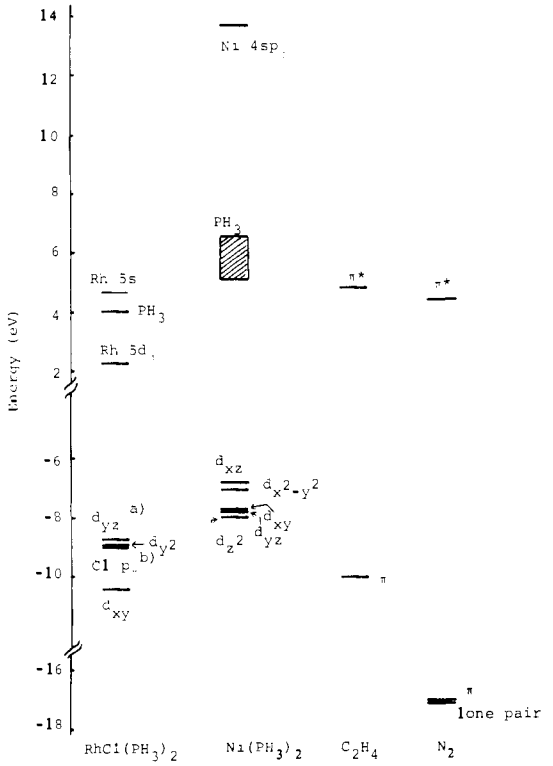

Figure 7. Orbital energy levels of $RhCl(PH_3)_2$ and $Ni(PH_3)_2$ near HOMO and LUMO: (a) antibonding coupling between Rh d_{yz} and Cl p_π, (b) bonding interaction between Rh d_{yz} and Cl p_π. See ref 18c for the MO calculation of $Ni(PH_3)_2$.

are given at several Rh–C_2H_4 distances in Figure 6, and they are connected as "reference curves", as examined above. The energy components of $Ni(PH_3)_2(C_2H_4)$, previously calculated,[18c] are plotted in this figure (marked by "●") at the Rh–C_2H_4 interfragment distance giving the same EX value as that of the Ni–C_2H_4 complex. Apparently, the BCTPLX stabilization of the Ni(0) complex is much larger but the FCTPLX stabilization is much less than that corresponding to the Rh–C_2H_4 complex. Some molecular orbitals near HOMO and LUMO of metal fragments are shown in Figure 7. The HOMO ($d\pi$) of $Ni(PH_3)_2$ lies higher in energy than that of $RhCl(PH_3)_2$, whereas their orbital energies are not so different. However, the acceptor orbital (Ni $4sp_\sigma$) of $Ni(PH_3)_2$ is placed at a substantially high energy level, leading to a very weak σ-donative interaction, but the LUMO (acceptor orbital) of $RhCl(PH_3)_2$ lies relatively low in energy, yielding a considerable σ-donative interaction.

In summary, $RhCl(PH_3)_2$ possesses the HOMO at a relatively high energy level and the LUMO at a relatively low energy level. Therefore, $RhCl(PH_3)_2$ can form both strong donative and back-donative interactions. In this regard, Rh(I) can be described as a versatile metal ion for the wide range of ligands. In contrast, $Ni(PH_3)_2$ has its HOMO and the acceptor orbital at a much higher energy level and, consequently, can form only a strong back-donative interaction. In other words, only a ligand possessing a good acceptor orbital can coordinate with Ni(0) to form the complex.

Conclusion

First, two coordination modes of N_2, η^1-end-on and η^2-side-on, were investigated in $RhCl(PH_3)_2(N_2)$. Both η^1-end-on and η^2-side-on coordination modes receive a similar degree of BCTPLX stabilization, but the η^2-side-on mode has weaker ES and FCTPLX interactions than the η^1-end-on mode does. The difference in ES interaction between the η^1-end-on and η^2-side-on modes results from the negative quadrupole moment of N_2; when the positively charged Rh(I) approaches to N_2 along the N-N axis to form the η^1-end-on N_2 complex, the large ES stabilization is caused by the negative quadrupole moment of N_2, but, when the Rh(I) approaches to N_2 perpendicularly to the N–N axis, less ES stabilization is caused. The situation becomes different in the η^2-coordinating C_2H_4 complex; Because C_2H_4 has a positive quadrupole moment unlike N_2, large ES stabilization is yielded when the Rh(I) approaches C_2H_4 perpendicularly to the C=C bond. The weak donative interaction, FCTPLX, of the η^2-side-on N_2 complex is considered to result from the lesser expanse of the N_2 π-orbital than that of the N_2 lone-pair orbital and the more stable orbital energy of the N_2 π than of the C_2H_4 π-orbital. Consequently, the η^2-side-on N_2 complex becomes less stable than the η^1-end-on N_2 and C_2H_4 complexes.

Second, the electron distribution of the η^1-end-on Rh^I–N_2 complex was examined; the N_c atom is more negatively charged than the N_t atom, contrary to the expectation based on the orbital-mixing rule. Two factors, the orbital-mixing rule and the N_2 polarization caused by the positively charged central metal, would influence the N_2 electron distribution. The orbital mixing makes N_t more negatively charged than N_c, but the positive charge of the central metal makes N_c more negatively charged than N_t. Because two factors yield different effects on the electron distribution, the N_2 electron distribution is very sensitive to the kinds of metals and ligands. In the Rh^I–N_2 complex, the effect of polarization is large, and, therefore, N_c becomes more negatively charged than N_t. The N 1s ionization energy was also studied. It has been believed that the higher N 1s ionization potential is assigned to the N_c 1s ionization, suggesting that N_t is more negatively charged than N_c. In this work, the N_c 1s ionization is calculated to be higher in energy than the N_t 1s ionization in spite of the more negative charge of N_c. This higher N_c 1s ionization is probably due to the positively charged Rh atom and less relaxation energy. Thus, the higher N_c 1s ionization energy is not in conflict with the larger negative charge of N_c.

Then, the coordinate bonding nature of N_2 was compared with that of similar ligands such as CO, HCN, and HNC. The coordinate bond becomes weak in the order HNC > CO > HCN > η^1-end-on N_2. The weak η^1-end-on N_2 coordinate bond is considered to result from the small ES interaction and small donative interaction. In the η^1-end-on Rh^I–N_2 complex, therefore, the relative importance of back-donation to the donation is larger than in the other complexes.

Finally, the versatile ability of Rh(I) for the ligand coordination is discussed in comparison with the Ni(0) complex. The Rh(I) complex has the HOMO (Rh $4d\pi$) at a considerably higher energy level and the LUMO (Rh $4d\sigma$) at a considerably lower energy level, resulting in both strong donative and back-donative interactions. In contrast, the Ni(0) complex has both donor orbital (Ni $3d\pi$) and acceptor orbital (Ni $4sp_\sigma$) at a considerably higher energy level. Thus, only a ligand possessing a good acceptor orbital can ligate to Ni(0). In this regard, Rh(I) has a versatile ability for coordination of various ligands.

Acknowledgment. We thank Dr. N. Kosugi (Tokyo University) for his kind helps of RHF calculations. S.S. is grateful for support through IMS Joint Studies Program and a Ministry of Education grant. Numerical calculations were carried out at the IMS Computer Center.

Registry No. $RhCl(PH_3)_2(\eta^1\text{-}N_2)$, 95344-48-2; $RhCl(PH_3)_2(\eta^2\text{-}N_2)$, 95344-49-3; $RhCl(PH_3)_2(C_2H_4)$, 95344-50-6; $RhCl(PH_3)_2(CO)$, 58201-16-4; $RhCl(PH_3)_2(HNC)$, 95344-51-7; $RhCl(PH_3)_2(HCN)$, 95344-52-8; $RhCl(PH_3)_2(NH_3)$, 95344-53-9; N_2, 7727-37-9; Rh, 7440-16-6.

(37) The usual 4-31G basis set was used for ligand atoms and the [4s3p2d] contracted basis set was used for Ni. See ref 18c for detailed discription.